

**CIRCUMSTELLAR AND INTERSTELLAR MATERIAL IN VOLATILE-RICH CLASTS FROM ACHONDRITIC KAPOETA METEORITE.** N. Liu<sup>1</sup> and R. C. Ogliore<sup>1</sup>, <sup>1</sup>Department of Physics, Washington University in St. Louis, St. Louis, MO 63130, USA, [nliu@physics.wustl.edu](mailto:nliu@physics.wustl.edu).

**Introduction** Howardites are achondritic breccia meteorites from Vesta [1], which contain carbonaceous chondrite clasts (C clasts). C clasts likely originated as low-speed impactors into Vesta’s regolith soon after its formation in the early Solar System [2]. These volatile-rich clasts are samples of primitive Solar System solids that may be distinct from carbonaceous chondrite meteorites which fall to Earth in the present day. Previous studies showed that volatile-rich clasts in howardites have similarities to carbonaceous chondrites of petrologic type 2 and are mainly composed of fine-grained matrix material [2]. Fine-grained matrix is, in fact, the dominant host of presolar grains and organic matter (OM) in primitive chondrites. Extensive *in situ* survey in the literature has shown that the abundance of presolar grains and the isotopic composition of OMs vary widely among different classes, largely reflecting the degree of secondary processing (*e.g.*, aqueous alteration, thermal metamorphism) experienced by the hosting matrix [3,4]. Information on the abundances and isotopic compositions of presolar grains and OMs in volatile-rich clasts in the Kapoeta meteorite, therefore, can be used to probe the secondary processes that these volatile-rich clasts experienced on their parent bodies as well as on Vesta. Here we present NanoSIMS H, C, N, and O isotopic data for a number of volatile-rich C clasts from Kapoeta.

**Experiments:** We first obtained ~12,000 backscattered electron images (50  $\mu\text{m}$  field-of-view) of a thin section of the Howardite Kapoeta (USNM 6733 1) using custom large-area scanning software for a Tescan Mira3 FEG-SEM. We identified 15 C clasts 20–100  $\mu\text{m}$  in size and acquired energy dispersive X-ray maps of these clasts. We then carried out NanoSIMS C and O ion imaging measurements in 13 of the 15 identified clasts with a total analysis area of ~11,000  $\mu\text{m}^2$ . The results for four of the clasts were previously reported [5]. We searched for presolar grains using the L’Image software, and the identified C-anomalous grains were further characterized by acquiring their  $^{12}\text{C}^{14}\text{N}$ ,  $^{12}\text{C}^{15}\text{N}$ ,  $^{28}\text{Si}$ ,  $^{29}\text{Si}$ ,  $^{30}\text{Si}$  negative ion images in  $\sim 3 \times 3 \mu\text{m}$  areas. We also carried out semi-automated H, C, and N ion imaging analyses in two steps to characterize OM in three of the 13 clasts with a total analysis area of  $\sim 2,000 \mu\text{m}^2$ . The primary  $\text{Cs}^+$  beam was 100–150 nm in size for C, O, and N isotope and 200–250 nm for H isotope measurements.

**Results:** We identified zero O-anomalous and eight C-anomalous grains in the initial C and O isotope

measurements based on the identification criteria given in [6]. The N and Si isotope ratios of these eight grains that were obtained later show that (1) four grains with larger  $^{12}\text{C}/^{13}\text{C}$  anomalies are all Si-rich and thus confirmed as presolar SiC grains, and (2) the other four grains with smaller C anomalies are all Si-poor and most likely OM particles (*e.g.*, Fig. 1). As a result, our NanoSIMS analyses yielded an upper limit of 2 ppm for the presolar silicate abundance and  $59_{-26}^{+42}$  ppm for the presolar SiC abundance ( $1\sigma$  statistical errors).

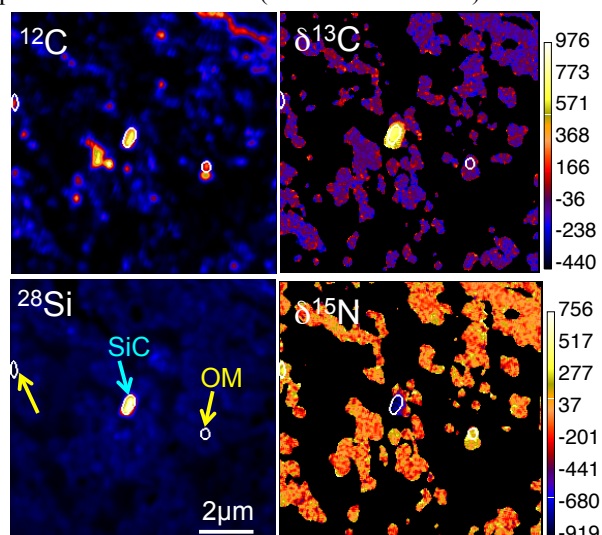


**Fig. 1.** Example NanoSIMS images of one  $10 \times 10 \mu\text{m}$  area in Kapoeta clast 042-002.

In addition, our H, C, N isotope imaging data show that the matrix materials in the three Kapoeta C clasts contain abundant Si-poor carbonaceous hotspots with both depletions and excesses in D,  $^{15}\text{N}$ , and  $^{13}\text{C}$ . We identified 48 H-, 3 C-, and 58 N-anomalous OM grains (Figs. 2, 3) based on the criteria that (1) the isotope ratio deviates from terrestrial values by  $>10\%$ , and (2) the isotopic anomaly is  $>3\sigma$ . All but one hotspot appear as single grains of 0.2 to 1.7  $\mu\text{m}$  in size and exhibit  $\delta\text{D}$  from protosolar ( $-870\text{‰}$ ) up to  $\sim 6000\%$  and  $\delta^{15}\text{N}$  from solar ( $-336\text{‰}$ ) up to  $\sim 1100\%$ . Carbon isotopic anomalies, on the other hand, are much rarer and smaller (Fig. 2). By assuming that the density of OMs is a factor of two lower than the matrix as a whole [7], we estimate an abundance of  $\sim 5,000$ ,  $\sim 200$ , and  $\sim 5,000$  ppm for H-, C-, and N-anomalous OM grains, respectively, with a mean  $\delta\text{D}$  and  $\delta^{15}\text{N}$  value of  $\sim 2000\text{‰}$  and  $\sim 200\text{‰}$ .

**Discussions:** The inferred abundances of presolar grains and OMs and their isotopic compositions from our study strongly support the inferred linkage between

volatile-rich clasts and fine-grained CI-, CM2-, and CR2-like materials from previous petrologic studies [e.g., 2]. In detail, the inferred presolar SiC abundance in these C-clasts is in good agreement with the abundance (~30 ppm) seen across primitive chondrite classes [8]. Although the inferred presolar silicate upper limit is lower than those reported for the majority of carbonaceous chondrites in the literature, it is consistent with the numbers for all CI, most CM2, and several CR2 meteorites [3], likely reflecting extensive O isotopic exchange with water during aqueous alteration. Because thermal metamorphism can result in loss of D enrichments in OMs from carbonaceous chondrites [e.g., 4], the preservation of D and  $^{15}\text{N}$  enrichments in the OMs implies that these volatile-rich C clasts did not experience significant heating neither on their parent body nor on Vesta, consistent with the low temperatures inferred from a recent Raman study [9]. The observed D and  $^{15}\text{N}$  enrichments (Fig. 3), however, are quite modest, which are more consistent with the low  $\delta\text{D}$  and  $\delta^{15}\text{N}$  enrichments observed in all CI and most CM chondrites than those in CR2 chondrites [4,10].

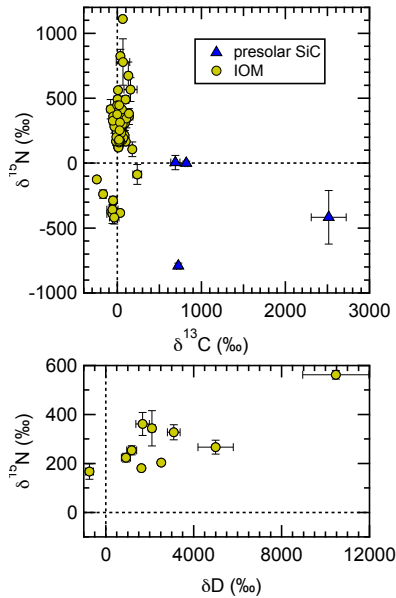


**Fig. 2.** C-N and N-H isotope plots of identified C- and/or N- anomalous grains. Errors are  $1\sigma$ .

Figure 2 shows that correlated D and  $^{15}\text{N}$  enrichments are only observed in ~20% of the N-anomalous OM grains (Fig. 2), consistent with the previous observation that the D and  $^{15}\text{N}$  hotspots do not always correlate with one another in primitive meteorites and IDPs. Given that volatile-rich clasts may have originated from different locations and at different times with respect to primitive meteorites and IDPs, the similarities in the abundances and isotopic compositions of OMs from these different extraterrestrial materials provide addi-

tional support to the proposal that OM compositional variations are caused by parent body processing of a common precursor [11].

Interestingly, we, for the first time, identified a few OM grains with the protosolar  $\delta\text{D}$  value (Fig. 3). These D “coldspots” are smaller (~300 nm in size) than the D hotspots observed in the same regions. As a result, our OM isotopic data points out an interesting fact that the lowest  $\delta\text{D}$  and  $\delta^{15}\text{N}$  values of the OM grains from this study both correspond to the solar/proto-solar values. The observed  $\delta\text{D}$  and  $\delta^{15}\text{N}$  enrichments, on the other hand, likely resulted from ion-molecule reactions at extremely low temperatures as proposed in the literature [4,10].

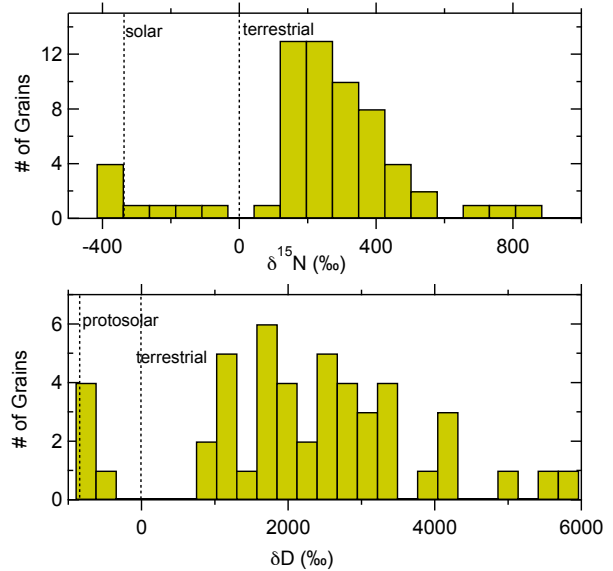


**Fig. 3.** Distributions of  $\delta\text{D}$  and  $\delta^{15}\text{N}$  values of the H- and N- anomalous grains identified in this study.

**Conclusions:** The abundances and isotopic compositions of presolar grains and OMs in volatile-rich clasts from Kapoeta obtained in this study confirm their linkage to CI- and CM-like materials inferred from previous petrologic studies. In addition, for the first time, we found several D-depleted OM “coldspots”. Their implications to the origin of OMs will be discussed at the meeting.

**References:** [1] Binzel, R. P. and Xu, S. (1993) *Sci.* 260, 186–191. [2] Gounelle M., et al. (1993) *GCA* 67, 507–527. [3] Floss, C. and Haenecour, P. (2016) *Geochem. J.* 50, 3–25. [4] Alexander, C. M. O’D., et al. (2007) *GCA*, 71, 4380–4403. [5] Liu, N. and Oglione, R. C. (2018) *MAPS* 81, #6151. [6] Floss, C. and Stadermann, F. J. (2012) *MAPS* 47, 992–1009. [7] Nittler, L. R., et al. (2018) *GCA* 226, 107–131. [8] Davidson, J., et al. (2014) *GCA* 139, 248–266. [9] Visser, R., et al. (2018) *GCA* 241, 38–55. [10] Busemann, H., et al. (2006) *Sci.* 312, 727–730. [11] Alexander, C. M. O’D., et al. (2012) *Sci.* 337, 721–723.